FEBS Letters 587 (2013) 3824–3830

journal homepage: www.FEBSLetters.org

Dynamic elements govern the catalytic activity of CapE, a capsular polysaccharide-synthesizing enzyme from *Staphylococcus aureus*

Takamitsu Miyafusa [a,b], Jose M.M. Caaveiro [a,b], Yoshikazu Tanaka [b,1], Kouhei Tsumoto [a,b,c,*]

[a] Medical Proteomics Laboratory, Institute of Medical Science, The University of Tokyo, Minato-ku, Tokyo 108-8639, Japan
[b] Department of Medical Genome Sciences, School of Frontier Sciences, The University of Tokyo, Minato-ku, Tokyo 108-8639, Japan
[c] Department of Chemistry and Biotechnology, School of Engineering, The University of Tokyo, Tokyo 113-8656, Japan

ARTICLE INFO

Article history:
Received 30 August 2013
Revised 3 October 2013
Accepted 11 October 2013
Available online 21 October 2013

Edited by Peter Brzezinski

Keywords:
Pathogenic bacterium
Capsular polysaccharide
X-ray crystallography
Conformational change
SDR enzyme
UDP-sugar
Staphylococcus aureus

ABSTRACT

CapE is an essential enzyme for the synthesis of capsular polysaccharide (CP) of pathogenic strains of *Staphylococcus aureus*. Herein we demonstrate that CapE is a 5-inverting 4,6-dehydratase enzyme. However, in the absence of downstream enzymes, CapE catalyzes an additional reaction (5-back-epimerization) affording a by-product under thermodynamic control. Single-crystal X-ray crystallography was employed to identify the structure of the by-product. The structural analysis reveals a network of coordinated motions away from the active site governing the enzymatic activity of CapE. A second dynamic element (the latch) regulates the enzymatic chemoselectivity. The validity of these mechanisms was evaluated by site-directed mutagenesis.

1. Introduction

The capsular polysaccharide (CP) of *Staphylococcus aureus* forms a thick layer of carbohydrate on the cell surface of the bacterium, conferring antiphagocytic properties, and helping *S. aureus* to persist in the bloodstream of the infected host. More than 70% of clinical isolates of *S. aureus* belong to either the CP5 or the CP8 serotypes [1,2]. Because the biosynthetic machinery that synthesizes CP in *S. aureus* is absent in humans, its inactivation constitutes an attractive strategy to fight this dangerous pathogen [2–4].

The conversion of UDP-D-GlcNAc into UDP-L-FucNAc (an essential precursor of CP) requires three enzymes CapE, CapF, and CapG in *S. aureus* [5–8]. CapE yields the first intermediate of the sequential reactions catalyzed by these three enzymes, although the mechanism is unclear [7,9]. CapE belongs to a distinctive subfamily of SDR enzymes of pathogenic bacteria characterized by a singular catalytic triad displaying a Met residue (instead of the canonical Tyr residue) and a dynamic element known as the latch [8]. The overall tertiary and quaternary structure of CapE is similar to the close homolog FlaA1 from *Helicobacter pylori* (identity 40%, rmsd = 2.0 ± 0.1 Å) [10,11]. Although CapE and FlaA1 afford the same product, the configuration of their active sites is different. Also, the latch region is absent in FlaA1. We sought to clarify the mechanism of CapE and to understand the functional impact of the dynamic regions in its enzymatic activity.

We report that CapE catalyzes the 5-inverting 4,6-dehydration reaction of substrate UDP-D-GlcNAc, followed by a slower 5-back-epimerization. The second reaction generates an irreversible by-product of unclear biological significance that is not processed by the downstream enzyme CapF. The crystal structure of CapE soaked with the substrate UDP-D-GlcNAc revealed the identity of the by-product, and structural elements regulating its reactivity. Site-directed mutagenesis validates the structural analysis.

2. Materials and methods

2.1. Enzymatic assay

The enzymatic activity of CapE, purified as described elsewhere [6,7], was monitored by the method described in Miyafusa et al.

Abbreviations: CP, capsular polysaccharide; SDR, short-chain dehydrogenase/reductase; SEC, size-exclusion chromatography; HPLC, high performance liquid chromatography; UDP-*arabino*-sugar, UDP-2-acetamido-2,6-deoxy-α-L-*arabino*-4-hexulose; UDP-*xylo*-sugar, UDP-2-acetamido-2,6-deoxy-α-D-*xylo*-4-hexulose

* Corresponding author at: Department of Medical Genome Sciences, School of Frontier Sciences, The University of Tokyo, Minato-ku, Tokyo 108-8639, Japan. Fax: +81 4 7136 3601.
E-mail address: tsumoto@ims.u-tokyo.ac.jp (K. Tsumoto).
[1] Present address: Creative Research Initiative Sousei, Hokkaido University, Sapporo 001-0021, Japan.

0014-5793/$36.00
http://dx.doi.org/10.1016/j.febslet.2013.10.009

[7]. In a typical assay, 200 μM of substrate UDP-D-GlcNAc (Wako, Japan) was mixed with 2 μM CapE in 20 mM Tris/HCl (pH 8.0) in a total volume of 100 μl at 37 °C. The reaction was stopped by adding 100 μl of ice-cold phenol/chloroform/isoamyl alcohol in a 25:24:1 M ratio. The supernatants containing the sugars were mixed with 100 μl of chloroform and analyzed by HPLC using a CarboPac PA1 anion-exchange column (Dionex) as described previously [12]. Filtrates of the reaction products after one-hour reaction where obtained by filtration through a Microcon YM-10 (Millipore), re-incubated with enzymes, and analyzed by HPLC.

2.2. Protein crystallization

Purified CapE was dialyzed in 10 mM Tris/HCl (pH 9.0), 30 mM NaCl, and 1 mM DTT, and concentrated with a 100 kDa Centriprep filtration unit (Millipore) prior to crystallization. Crystallization was carried out as described for wild-type protein in the substrate-free form [8]. Suitable crystals were soaked in mother liquor supplemented with 25% (v/v) glycerol and 500 μM UDP-D-GlcNAc.

2.3. Data collection and refinement

Crystals of CapE were mounted under a stream of cold nitrogen (100 K) at beamline BL5A of the Photon Factory (Tsukuba, Japan). Diffraction data were processed with the program MOSFLM [13] and merged and scaled using the program SCALA of the CCP4 program suite [14]. The structure was determined by the method of molecular replacement with the program PHASER [15]. Refinement was carried out with REFMAC5 [16] and COOT [17]. Model quality was assessed with PROCHECK [18]. Data collection and refinement statistics are given in Table 1.

Table 1
Data collection and refinement statistics.

	CapE with by-product
Data collection	
Space group	$P6_322$
Unit cell	
Dimensions (Å)	$a = b = 124.03$, $c = 103.16$
Angles (°)	$\alpha = \beta = 90$, $\gamma = 120$
Wavelength (Å)	1.0000
Resolution range (Å)	35.8–1.88
Total observations	292 144
Unique observations	38 463
I/σ (I)	12.5 (2.4)
Completeness (%)	99.9 (99.9)
R_{merge}[a] (%)	11.0 (88.7)
Multiplicity	7.6 (7.6)
Refinement	
R_{work}/R_{free}[b] (%)	17.5/20.9
No. protein chains	1
No. protein residues	346
No. protein atoms	2722
No. ligands	18
No. ligand atoms	167
No. water molecules	136
B-factor, protein (Å^2)	37.8
B-factor, ligands (Å^2)	51.8
B-factor, water (Å^2)	37.9
RMSD bonds (Å)	0.024
RMSD bonds (°)	2.46
Coordinate error (Å)	0.12
Ramachandran plot	
Preferred regions (%)	97.4
Allowed regions (%)	2.6
Outliers (%)	0.0
PDB code	4G5H

Values in parenthesis correspond to the highest resolution bin.
[a] $R_{merge} = \Sigma_{hkl} \Sigma_i |I(hkl)_i - [I(hkl)]| / \Sigma_{hkl} \Sigma_i I(hkl)$.
[b] $R_{work} = \Sigma_{hkl} |F(hkl)_o - [F(hkl)_c]| / \Sigma_{hkl} F(hkl)_o$; R_{free} was calculated as R_{work}, where $F(hkl)_o$ values were taken from 5% of data not included in the refinement.

3. Results and discussion

3.1. Catalytic mechanism of CapE

The enzymatic activity of CapE on its natural substrate UDP-D-GlcNAc affords two different products (Fig. 1A). Previous efforts to identify the nature of each one were unsuccessful [7,8]. The time course of the reaction shows that the two products do not appear simultaneously, but sequentially (Fig. 1B). After 30 min the product displaying the fast kinetic component exceeds the product with the slow kinetic component by a ratio of 2:1. However, after three hours their relative abundance is reversed: the amount of slow product exceeds that of the fast-appearing product by ~9-fold. Comparable observations are reported for three homologous enzymes of CapE, namely WbjB from *Pseudomonas aeruginosa* (67% identity), FlaA1 from *Helicobacter pylory* (40% identity), and PseB from *Campylobacter jejuni* (41% identity) [19–21]. Based on the identity of the reaction products reported for these homologous proteins (mechanistically identical to each other) we propose that the compound generated in the first reaction is UDP-2-acetamido-2,6-deoxy-α-L-*arabino*-4-hexulose (UDP-*arabino*-sugar). This product is obtained after the 5-inverting 4,6-dehydration reaction. The second compound corresponds to the 5-back-epimerization of the UDP-*arabino*-sugar, i.e. UDP-2-acetamido-2,6-deoxy-α-D-*xylo*-4-hexulose (UDP-*xylo*-sugar). We acquired ^{1}H NMR spectra of the reaction products at various intervals to confirm their identity. This experiment shows that UDP-*arabino*-sugar and UDP-*xylo*-sugar are generated in a sequential manner, analogously to the time-course analysis by HPLC above (Supplementary Fig. S1) [19].

To verify this mechanism, the mixture of the two compounds produced by CapE were purified by a filtration method [9], and re-incubated with enzymes CapE and CapF under various conditions (Fig. 1C). The two compounds do not react unless CapE is present (compare curve I and II). Importantly, the downstream enzyme CapF processes only UDP-*arabino*-sugar (curve III). This key observation indicates that the other compound, UDP-*xylo*-sugar, is a by-product in the context of this biosynthetic route. In contrast, when CapE and CapF are both incubated with substrate UDP-D-GlcNAc the reaction proceeds without detectable formation of by-product (curve IV). From the concentration-dependence curve it is further demonstrated that CapE catalyzes the 5-back-epimerization side-reaction (Fig. 1D). These results are consistent with the scheme shown in Fig. 1E.

The yield of by-product afforded by CapE is substantially higher than that catalyzed by FlaA1 or PseB [10,21], despite employing less than one-tenth concentration of CapE and substrate than that described for the other homologous enzymes [10]. The idiosyncratic environment of the active site of CapE and its dynamic elements such as the latch [8] may explain the higher yields of by-product (see below).

3.2. Crystal structure of CapE in complex with by-product

Crystals of holo-CapE were grown as previously reported [8] and soaked with substrate UDP-D-GlcNAc. The high concentration of enzyme in the crystal (~10 mM) ensures a rapid conversion to products. Crystals diffracted to a resolution of 1.88 Å, revealing several molecules bound to the CapE: coenzyme NADPH/NADP$^+$, UDP-*xylo*-sugar (by-product) in the active site, and a UDP-sugar at an unexpected binding pocket (Fig. 2). Overall, the structure of CapE is virtually identical to that of apo-CapE in complex with a substrate analog (PDB code 3W1V; rmsd = 0.41 Å) [8]. The dynamic region known as the latch (residues 287–309) occupies the same

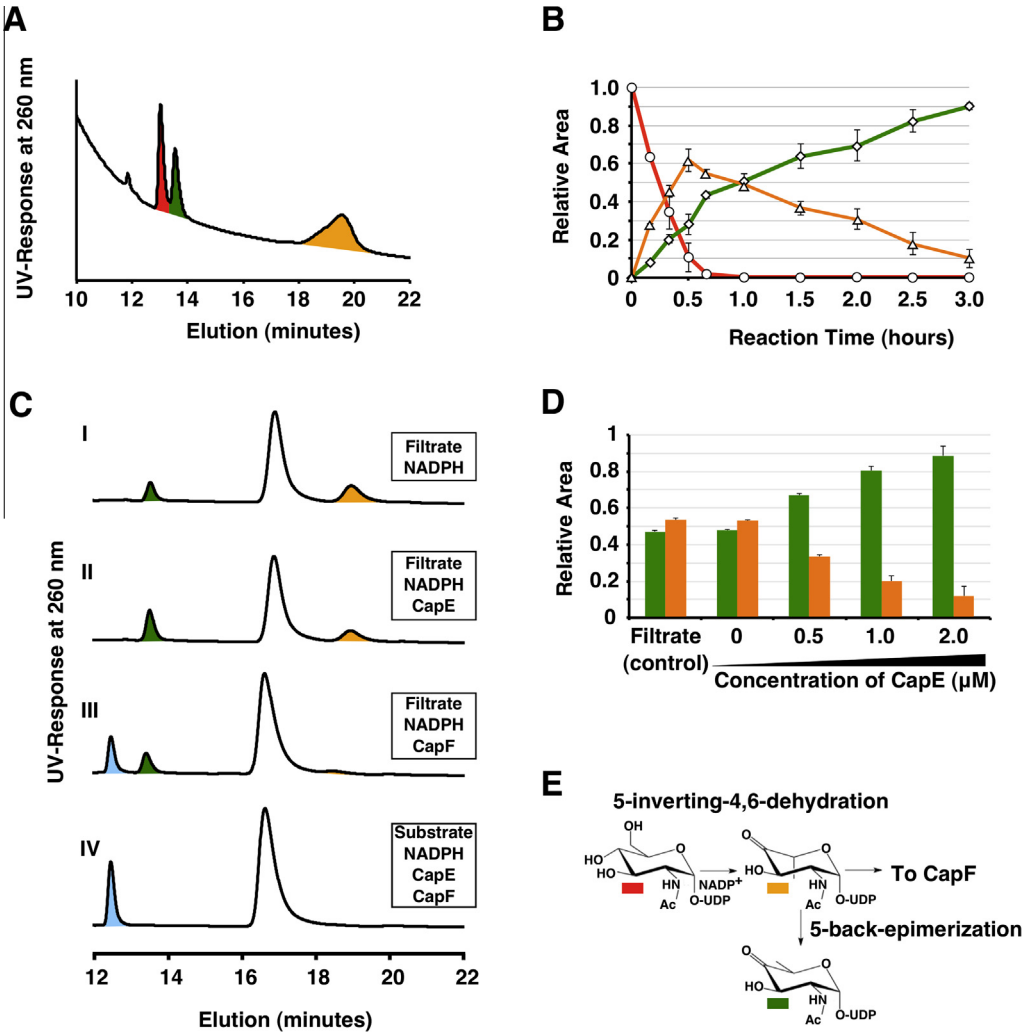

Fig. 1. Mechanism of CapE. (A) HPLC profile after incubation substrate UDP-D-GlcNAc (200 μM) with CapE (2 μM) for 20 min. The peak of substrate (UDP-D-GlcNAc), product (UDP-*arabino*-sugar), and by-product (UDP-*xylo*-sugar) are shown in red, orange and green, respectively. (B) Time-course of the reaction. (C) HPLC profiles of product filtrates incubated with NADPH (curve I), with NADPH and CapE (curve II), with NADPH and CapF (curve III). Curve IV represents a control experiment using NADPH, CapE, CapF, and UDP-D-GlcNAc (no filtrates). NADPH is required for the activity of CapF. The peak corresponding to the product of CapF (UDP-2-acetamido-2,6-dideoxy-β-L-talose) is shown in blue. (D) Reaction of product filtrates with increasing concentrations of CapE. (E) Reaction scheme.

position in both structures. Because the latch was not observed in holo-CapE [8] we conclude that its structuring is coupled to the binding of UDP-sugar, but not to the binding of coenzyme [8]. We note that, in the crystal, the active site of CapE is accessible to the solvent and does not form part of crystal-packing contacts. In addition, the structure of substrate-free CapE have previously demonstrated the possibility of very large conformational changes of the catalytic domain in the crystal form [8], thus enabling enzymatic activity.

The structure of CapE also reveals the identity of the molecule bound to the active site, UDP-*xylo*-sugar. This compound is the by-product generated in the second reaction (Fig. 3). The by-product is anchored to the protein by non-covalent interactions through its UDP moiety (Supplementary Table 1). The hexose ring occupies a non-catalytic conformation with respect to the coenzyme. The C4 atom of the nicotinamide ring of the coenzyme and the C4′ atom of the sugar are separated by 6.3 Å, a distance too large for the reaction to proceed [22]. The same binding conformation is observed in the crystal structure of CapE with substrate analog bound [8], and FlaA1 in complex with UDP-D-Gal (Supplementary Fig. S2) [10]. The exact role of this inactive conformation is unclear. We propose that Leu86 acts as a quality-control gatekeeper blocking the release of the hypothetical C3-epimerized by-product from the enzyme (Fig. 3D). The distance between the CG atom of Leu86 and the O3 atom of the hexose ring is 3.7 Å in the crystal structure. However, the hypothetical epimerization of the C3 would lead to unfavorable steric clashes between the sugar ring and Leu86, thus disfavoring the C3 epimerization route.

We note that a second molecule of UDP-sugar is found at a novel binding pocket remote from the active site (Fig. 2A and D). The identity of the hexose ring could not be determined because of dynamic disorder. The interaction between Tyr 305 and the UDP moiety suggests that the secondary binding site stabilizes the conformation of the latch and may play a role in the enzymatic regulation of CapE as observed in other enzymes [23].

3.3. Coordinated motion of hydrophobic side chains near the coenzyme

Residues Phe16, Phe78, Leu122 and Tyr164 of the coenzyme binding domain show clear signs of static disorder (Fig. 4; Supplementary Fig. S3). This observation contrasts with the single conformation of the same residues in the structure of holo-CapE (PDB code 3VVC) [8]. We employed the software RINGER [24] to evalu-

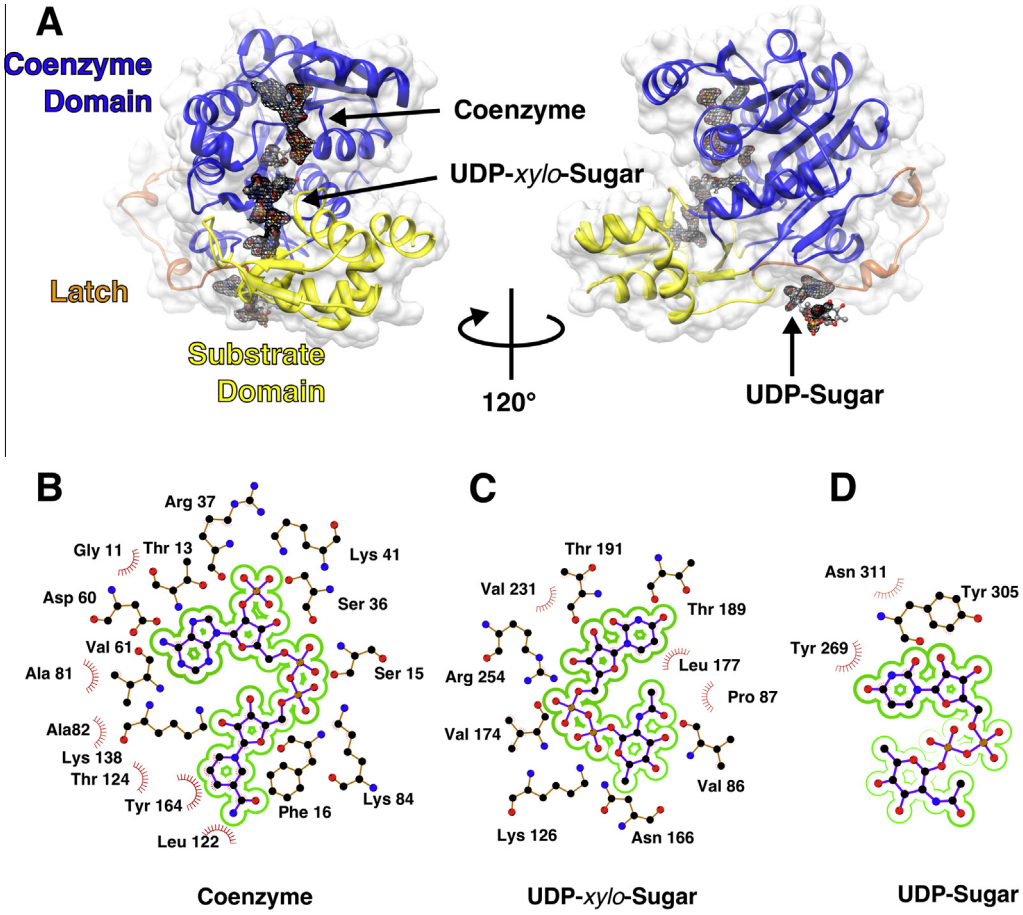

Fig. 2. Structure of CapE. (A) Overall conformation of wild-type CapE soaked with substrate. UDP-*xylo*-sugar is found at the active site. A second UDP-sugar is found at a novel secondary binding site. The hexose ring of the second UDP-sugar is disordered and could not be modeled. The substrate binding domain, the coenzyme binding domain, and the *latch* are colored in blue, yellow, and orange, respectively. Ligands are depicted as ball and sticks with CPK colors. The sigma-A weighted omit difference electron density maps ($F_o - F_c$) of the ligands are contoured at 2.5 σ. The bottom panels represent the binding environment of (B) coenzyme, (C) by-product (active site), and (D) UDP-sugar (at the secondary binding site). B–D were generated with the program LIGPLOT [29].

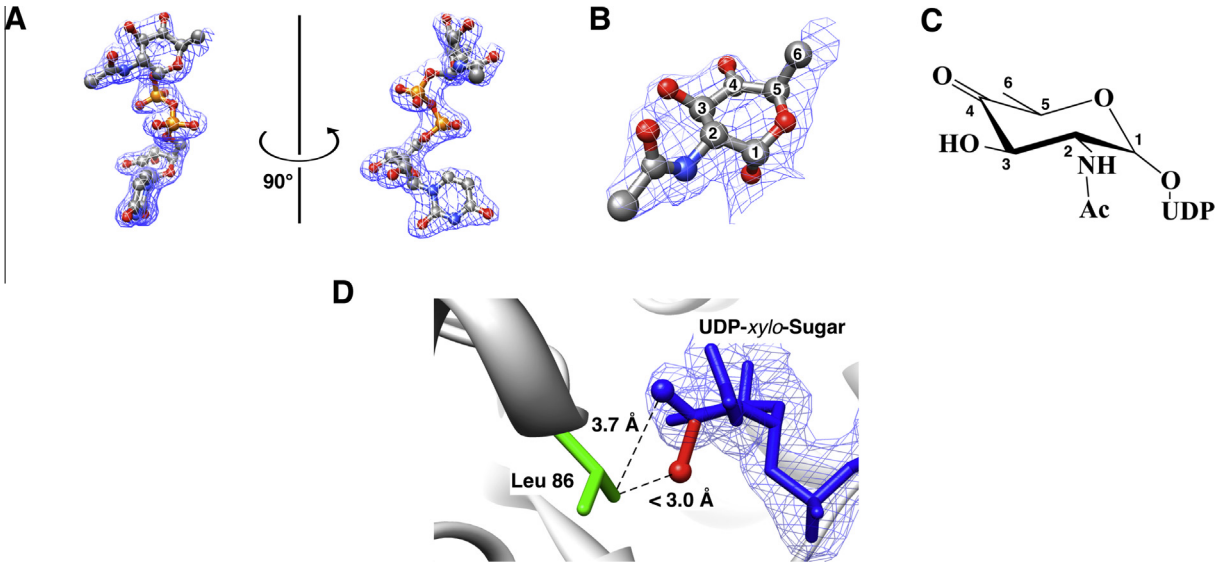

Fig. 3. Structure of by-product. (A) UDP-*xylo*-sugar is depicted as ball and sticks with CPK colors. The sigma-A weighted omit difference electron density maps ($F_o - F_c$) of the UDP-*xylo*-sugar is contoured at 2.5 σ. (B) Close-up view of hexose ring. (C) Chemical structure of the hexose ring. (D) Structure of Leu86 (green) near the O3 atom of the hexose ring (blue). The hydroxyl group of the hypothetically epimerized C3 atom of the UDP-sugar (red) would clash with the OG atom of Leu86 in this conformation.

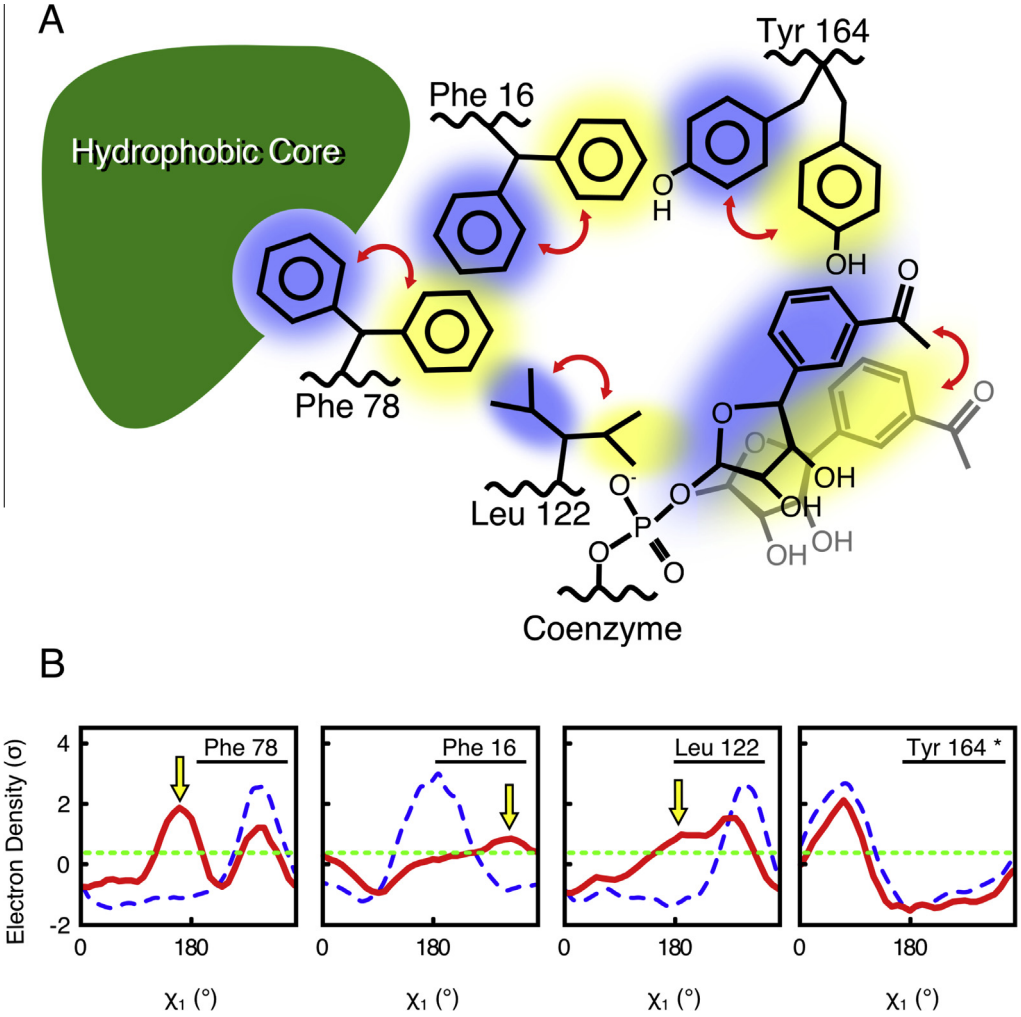

Fig. 4. Flap region. The binding of substrate induces coordinated motions in hydrophobic residues adjacent to the coenzyme. (A) Schematic representation of the coordinated changes in side-chains of Phe16, Phe78, Leu122 and Tyr164. The *in-conformer* (facing the hydrophobic core), and the *out-conformer* (facing the coenzyme) are highlighted with blue and yellow shades, respectively. The red arrows indicate coordinated motions. The *out*-conformer of the coenzyme it is colored in gray to indicate disorder. (B) Electron density plots calculated with RINGER [24]. Dashed line (blue) corresponds to the electron density level of holo-CapE (PDB code 3VVC). Red line corresponds to that of CapE in complex with UDP-sugar. Yellow arrows indicate the new conformation sampled in the structure with UDP-sugar. No differences were observed in the plot of Tyr164 because the conformational change occurs in the backbone of this residue (not in the side-chain).

ate quantitatively the relative fraction of each rotamer (Fig. 4B). The analysis reveals that the side chain of Phe78 displays two conformations populated at angles of 170° and 320° in the structure with UDP-*xylo*-sugar bound, but only one conformer ($\chi_1 = 320°$) in the substrate-free structure. The *in-rotamer*, which populates both structures, points its side chain towards the hydrophobic core of the protein. The *out-rotamer*, only present in the sugar-bound form, faces the coenzyme moiety.

The coupled motions of this region (*flap* region) are caused by a conformational relay mechanism that connects the hydrophobic core of the enzyme with the coenzyme. The reorientation of Phe78 triggers alternate conformations in Phe16, Leu122, and Tyr164. The *out-conformer* of Tyr164 is not identified by the program RINGER because it involves reconfiguration of the main-chain atoms, but not the side-chain. Lastly, the movement of Tyr164 pushes the nicotidamine moiety of the coenzyme out of its position towards an inactive conformation. Consequently the occupancy of the nicotidamine is reduced to 50%, although the second conformation cannot be modeled because of disorder. The disorder in the nicotidamine moiety of the coenzyme clearly contrasts with the ordered conformation in its adenosine moiety.

Dynamic features in the coenzyme region are observed in other SDR enzymes. For example, changes in the conformation of NADPH are required for specificity in guanosine monophosphate reductase [25]. Similar examples are described for the dehydrogenase domain of ArnA [26], and CapF [7]. In the case of CapE, we speculate that the movement of the coenzyme assists the rearrangement and eventual exit of the product.

3.4. Site-directed mutagenesis validates the structural findings

We prepared mutants of CapE to validate the mechanism discussed above (Fig. 5). The enzymatic activity of mutein Y164F (belonging to the flap) is unchanged with respect to wild type protein (Fig. 5A), demonstrating that Tyr164 does not act as the general base as it does in SDR enzymes displaying the SYK triad motif [27,28]. In contrast, the activity of mutein Y164A decreased dramatically in comparison with wild-type protein, indicating that the function of Tyr 164 is related to its bulkiness in the relay mechanism explained above.

We also mutated residues Phe78 and Leu122 to Trp and Phe, respectively, with the idea of blocking the cooperative conformational change of hydrophobic side chains. Whereas the consumption of substrate of mutein L122F decreases substantially with respect to wild-type protein, that of mutein F78W does not change significantly (Fig. 5A and B, Supplementary Table S2). Other

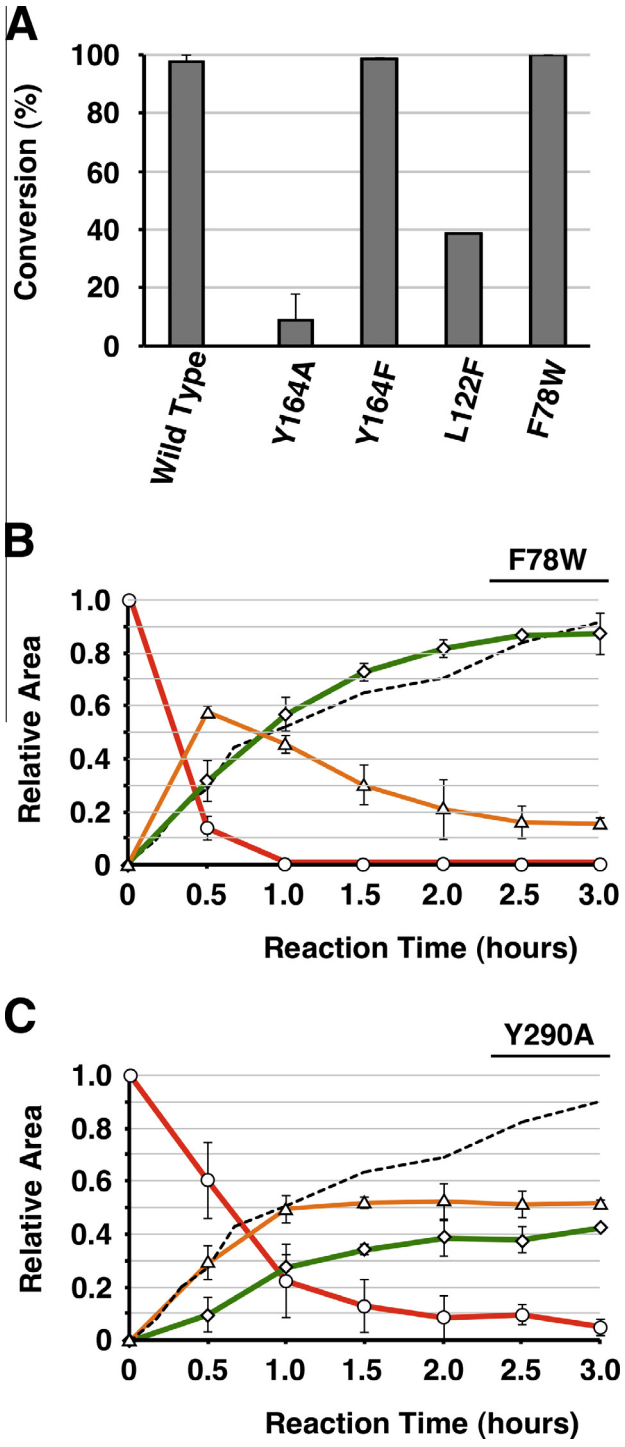

Fig. 5. Mutational analysis. (A) Wild type CapE or muteins (2 μM) were incubated with UDP-D-GlcNAc (200 μM) for 2 h at 37 °C. The consumption of substrate UDP-D-GlcNAc was monitored by HPLC. The bars correspond to the average of three independent assays ± standard deviation. Time-course curve of (B) mutein F78W (flap region), and (C) mutein Y290A (latch region). The relative amount of UDP-*xylo*-sugar catalyzed by wild type enzyme is also shown (dotted line).

techniques such as molecular dynamics simulations will be required to further reveal the operating mechanism at this region.

A second dynamic element of CapE is the latch [8]. Previously we showed that altering the latch by site-directed mutagenesis increases the ratio of UDP-*arabino*-sugar with respect to UDP-*xylo*-sugar [8]. The time course of the reaction catalyzed by a new mutation in the latch (Y290A) corroborates previous observations (Fig. 5C). This mutation reduces the enzymatic activity of CapE and reverses the yield of product with respect to by-product. In other words, the structural and kinetic data indicates that the latch region is important for the activity and chemoselectivity of CapE by adjusting the relative position between the substrate biding domain and the coenzyme biding domain.

4. Conclusion

It is shown that CapE catalyzes two sequential reactions, 5-inverting 4,6-dehydration followed by the 5-back-epimerization side-reaction. The second reaction does not occur in the presence of the downstream protein CapF because this enzyme consumes the product of the first reaction faster than the time-scale of the 5-back epimerization. High-resolution X-ray structure was employed to reveal the nature of the by-product (UDP-*xylo*-sugar). Unexpectedly, a molecule of UDP-sugar was found bound to a novel pocket in a location remote form the active site. We identified key dynamic regions governing the catalytic activity and the yield of product with respect to by-product. We hope this information is useful for the design of novel drugs of high potency and specificity.

Author conribution

Takamitsu Miyafusa and Jose M.M. Caaveiro designed research, performed experiments, analyzed data, and wrote the manuscript. Yoshikazu Tanaka performed experiments. Kouhei Tsumoto designed research and analyzed data. All authors approved the manuscript.

Accession Codes

Atomic coordinates and structure factors of CapE in complex with UDP-*xylo*-sugar and NADPH are deposited in the PDB under entry code 4G5H.

Funding

This work was supported in part by a Grant-in-Aid for General Research from the Japan Society for the Promotion of Science (to K.T.). The funding agency had no role in the design of the study, the collection, analysis and interpretation of the data, the writing of the report, and in the decision to submit the manuscript for publication.

Acknowledgements

We appreciate useful suggestions from Dr. M. Yao (Hokkaido University). Access to beamlines AR-NE3A and BL5A was granted by the Photon Factory Advisory Committee (Proposal Numbers 2009G204 and 2011G574).

Appendix A. Supplementary data

Supplementary data associated with this article can be found, in the online version, at http://dx.doi.org/10.1016/j.febslet.2013.10.009.

References

[1] Luong, T.T. and Lee, C.Y. (2006) The arl locus positively regulates *Staphylococcus aureus* type 5 capsule via an mgrA-dependent pathway. Microbiology (SGM) 152, 3123–3131.
[2] Luong, T.T. and Lee, C.Y. (2002) Overproduction of type 8 capsular polysaccharide augments *Staphylococcus aureus* virulence. Infect. Immun. 70, 3389–3395.
[3] O'riordan, K. and Lee, J.C. (2004) *Staphylococcus aureus* capsular polysaccharides. Clin. Microbiol. Rev. 17, 218–234.

[4] Watts, A., Ke, D.B., Wang, Q., Pillay, A., Nicholson-Weller, A. and Lee, J.C. (2005) *Staphylococcus aureus* strains that express serotype 5 or serotype 8 capsular polysaccharides differ in virulence. Infect. Immun. 73, 3502–3511.
[5] Kneidinger, B., O'Riordan, K., Li, J., Brisson, J.R., Lee, J.C. and Lam, J.S. (2003) Three highly conserved proteins catalyze the conversion of UDP-N-acetyl-D-glucosamine to precursors for the biosynthesis of O antigen in Pseudomonas aeruginosa O11 and capsule in *Staphylococcus aureus* type 5. Implications for the UDP-N-acetyl-L-fucosamine biosynthetic pathway. J. Biol. Chem. 278, 3615–3627.
[6] Miyafusa, T., Tanaka, Y., Kuroda, M., Ohta, T. and Tsumoto, K. (2008) Expression, purification, crystallization and preliminary diffraction analysis of CapF, a capsular polysaccharide-synthesis enzyme from *Staphylococcus aureus*. Acta Crystallogr., Sect. F: Struct. Biol. Cryst. Commun. 64, 512–515.
[7] Miyafusa, T., Caaveiro, J.M.M., Tanaka, Y. and Tsumoto, K. (2012) Crystal structure of the enzyme CapF of *Staphylococcus aureus* reveals a unique architecture composed of two functional domains. Biochem. J. 443, 671–680.
[8] Miyafusa, T., Caaveiro, J.M., Tanaka, Y., Tanner, M.E. and Tsumoto, K. (2013) Crystal structure of the capsular polysaccharide synthesizing protein CapE of *Staphylococcus aureus*. Biosci. Rep. 33, 463–474.
[9] Mulrooney, E.F., Poon, K.K.H., McNally, D.J., Brisson, J.R. and Lam, J.S. (2005) Biosynthesis of UDP-N-acetyl-L-fucosamine, a precursor to the biosynthesis of lipopolysaccharide in *Pseudomonas aeruginosa* serotype O11. J. Biol. Chem. 280, 19535–19542.
[10] Ishiyama, N., Creuzenet, C., Miller, W.L., Demendi, M., Anderson, E.M., Harauz, G., Lam, J.S. and Berghuis, A.M. (2006) Structural studies of FlaA1 from *Helicobacter pylori* reveal the mechanism for inverting 4,6-dehydratase activity. J. Biol. Chem. 281, 24489–24495.
[11] Creuzenet, C., Urbanic, R.V. and Lam, J.S. (2002) Structure-function studies of two novel UDP-GlcNAc C6 dehydratases/C4 reductases. Variation from the SYK dogma. J. Biol. Chem. 277, 26769–26778.
[12] Oka, T., Nemoto, T. and Jigami, Y. (2007) Functional analysis of Arabidopsis thaliana RHM2/MUM4, a multidomain protein involved in UDP-D-glucose to UDP-L-rhamnose conversion. J. Biol. Chem. 282, 5389–5403.
[13] Leslie, A.G. (2006) The integration of macromolecular diffraction data. Acta Crystallogr. D Biol. Crystallogr. 62, 48–57.
[14] Evans, P. (2006) Scaling and assessment of data quality. Acta Crystallogr. D Biol. Crystallogr. 62, 72–82.
[15] McCoy, A.J., Grosse-Kunstleve, R.W., Storoni, L.C. and Read, R.J. (2005) Likelihood-enhanced fast translation functions. Acta Crystallogr. D Biol. Crystallogr. 61, 458–464.
[16] Murshudov, G.N., Vagin, A.A. and Dodson, E.J. (1997) Refinement of macromolecular structures by the maximum-likelihood method. Acta Crystallogr. D Biol. Crystallogr. 53, 240–255.
[17] Emsley, P. and Cowtan, K. (2004) Coot: model-building tools for molecular graphics. Acta Crystallogr. D Biol. Crystallogr. 60, 2126–2132.
[18] Laskowski, R.A., Macarthur, M.W., Moss, D.S. and Thornton, J.M. (1993) Procheck—a program to check the stereochemical quality of protein structures. J. Appl. Crystallogr. 26, 283–291.
[19] McNally, D.J., Schoenhofen, I.C., Mulrooney, E.F., Whitfield, D.M., Vinogradov, E., Lam, J.S., Logan, S.M. and Brisson, J.R. (2006) Identification of labile UDP-ketosugars in *Helicobacter pylori*, *Campylobacter jejuni* and *Pseudomonas aeruginosa*: key metabolites used to make glycan virulence factors. ChemBioChem 7, 1865–1868.
[20] Schoenhofen, I.C., McNally, D.J., Vinogradov, E., Whitfield, D., Young, N.M., Dick, S., Wakarchuk, W.W., Brisson, J.R. and Logan, S.M. (2006) Functional characterization of dehydratase/aminotransferase pairs from helicobacter and campylobacter – enzymes distinguishing the pseudaminic acid and bacillosamine biosynthetic pathways. J. Biol. Chem. 281, 723–732.
[21] Morrison, J.P., Schoenhofen, I.C. and Tanner, M.E. (2008) Mechanistic studies on PseB of pseudaminic acid biosynthesis: a UDP-N-acetylglucosamine 5-inverting 4,6-dehydratase. Bioorg. Chem. 36, 312–320.
[22] Beis, K., Allard, S.T., Hegeman, A.D., Murshudov, G., Philp, D. and Naismith, J.H. (2003) The structure of NADH in the enzyme dTDP-D-glucose dehydratase (RmlB). J. Am. Chem. Soc. 125, 11872–11878.
[23] Peterson, A.W., Cockrell, G.M. and Kantrowitz, E.R. (2012) A second allosteric site in *Escherichia coli* aspartate transcarbamoylase. Biochemistry (US) 51, 4776–4778.
[24] Fraser, J.S., Clarkson, M.W., Degnan, S.C., Erion, R., Kern, D. and Alber, T. (2009) Hidden alternative structures of proline isomerase essential for catalysis. Nature 462, 669–673.
[25] Patton, G.C., Stenmark, P., Gollapalli, D.R., Sevastik, R., Kursula, P., Flodin, S., Schuler, H., Swales, C.T., Eklund, H., Himo, F., Nordlund, P. and Hedstrom, L. (2011) Cofactor mobility determines reaction outcome in the IMPDH and GMPR (β-α)(8) barrel enzymes. Nat. Chem. Biol. 7, 950–958.
[26] Gatzeva-Topalova, P.Z., May, A.P. and Sousa, M.C. (2005) Structure and mechanism of ArnA: conformational change implies ordered dehydrogenase mechanism in key enzyme for polymyxin resistance. Structure 13, 929–942.
[27] Jornvall, H., Hoog, J.O. and Persson, B. (1999) SDR and MDR: completed genome sequences show these protein families to be large, of old origin, and of complex nature. FEBS Lett. 445, 261–264.
[28] Kavanagh, K., Jornvall, H., Persson, B. and Oppermann, U. (2008) The SDR superfamily: functional and structural diversity within a family of metabolic and regulatory enzymes. Cell. Mol. Life Sci. 65, 3895–3906.
[29] Wallace, A.C., Laskowski, R.A. and Thornton, J.M. (1995) LIGPLOT: a program to generate schematic diagrams of protein-ligand interactions. Protein Eng. 8, 127–134.